Soil porosity in physically separated fractions and its role in SOC protection

Gianluca Simonetti[1] · **Ornella Francioso**[2] · **Nicola Dal Ferro**[1] · **Serenella Nardi**[1] ·
Antonio Berti[1] · **Francesco Morari**[1]

Abstract

Purpose Processes that lead to soil organic carbon (SOC) protection depend on both soil porosity and structure organization, as well as chemical and biological properties. In particular, the soil micro-nano porosity (<30 μm) regulates microorganism accessibility to the soil pore system and offers surfaces for organic carbon adsorption and intercalation into soil minerals. The aim of this work was to investigate how pore size distribution can selectively protect specific carbon pools in different aggregate size fractions, by considering the effects of long-term application of farmyard manure (FYM) and mineral (Min) fertilization.
Materials and methods Macroaggregates (250–2000 μm), microaggregates (53–250 μm), and silt–clay (<53 μm) fractions of three different soils (clayey, peaty, and sandy) were separated by wet sieving technique and then subjected to chemical and physical analysis. Sample porosity and pore size distribution were analyzed using mercury intrusion porosimetry (MIP), while SOC chemical structure was characterized by means of nuclear magnetic resonance (^{13}C cross-polarization–magic angle spinning nuclear magnetic reso-

nance (CP MAS ^{13}C NMR)) and diffuse reflectance infrared Fourier transform (DRIFT) spectroscopies.
Results and discussion Results showed that FYM increased organic (OC) and humic carbon (HC) content compared to the Min fertilization and unfertilized soils. However, it caused a gradual decrease in O,N-alkyl C, and alkyl C of humic C from macroaggregate to silt–clay fractions, suggesting an advanced state of humic component degradation as revealed by CP MAS ^{13}C NMR, DRIFT analyses. MIP analysis showed a clear increase of micropores (5–30 μm) and cryptopores (0.0035–0.1 μm) from macroaggregate to silt–clay fractions, while minor differences were observed among the treatments. The application of principal component analysis to mineral soil fractions identified the formation of three main clusters, where (i) macroaggregates of clayey soil were mainly associated to cryptopores and OC and (ii) microaggregates and silt–clay fraction were mainly isolated by carbonyl C, ultramicropores, and total porosity. The third cluster was associated with medium and fine sand of the sand soil fraction as coupled with O,N-alkyl C, anomeric C, mesopores, and HC/OC ratio.
Conclusions Overall, this study indicates that pore size distribution may be a valuable indicator of soil capacity to sequester carbon, due to its direct influence on SOC linkages with soil aggregates and the positive effects against SOC decomposition phenomena. In this context, micropore- to nanopore-dominated structures (e.g., clayey soil) were able to protect OC compounds by interacting with mineral surfaces and intercalation with phyllosilicates, while meso/macropore-dominated structures (i.e., sandy soil) exhibited their low ability to protect the organic components.

✉ Gianluca Simonetti
gianluca.simonetti@unipd.it

[1] Dipartimento di Agronomia Animali Alimenti Risorse Naturali e Ambiente (DAFNAE), Università di Padova, Viale dell'Università 16-Agripolis, 35020 Legnaro, Padova, Italy

[2] Dipartimento di Scienze Agrarie, Università di Bologna, Viale Fanin 44, 40127 Bologna, Italy

1 Introduction

In the last decade, increasing attention has been given to the physical separation of soil organic carbon (SOC), aiming to obtain homogeneous pool fractions that are related to different stabilization mechanisms (Lützow et al. 2006). Many studies focused on aggregate stability and turnover (Six et al. 2002) since a complex feedback involves soil structure evolution and SOC turnover (Christensen 2001). On the one hand, SOC plays a pivotal role on aggregation mechanisms by acting as a binding agent between particles, but on the other, it is protected from microbial attack within soil pores (Dungait et al. 2012; Regelink et al. 2015). Indeed, SOC protection is promoted by the physical disconnection between decomposers and organic matter (Schmidt et al. 2011). The spatial distributions of SOC, solutes, and microbial communities within aggregates depend on the pore development within aggregates (Chenu et al. 2001; Kuka et al. 2007; Eusterhues et al. 2007) and pore interconnections that are accountable for the limited movement of microorganisms among their different size categories. Different authors (Hènaut et al. 2002; Edwards et al. 2007; Van Haastert and Bosgraaf 2009; Reynolds et al. 1989) described microorganism movements in the soil matrix as a "random walk," with a probability of access to organic matter that is mainly controlled by a combination of biological, physical, and chemical variables (Dungait et al. 2012). For this reason, the decomposers' ability to metabolize SOC is strongly regulated by pore size and their degree of connection.

Soil aggregation occurs through complex interactions of physical processes, chemical associations, and biological activity (Oades and Waters 1991; Jastrow and Miller 1998; Six et al. 2004). A simple hierarchical model for soil aggregation can explain many aspects of the dynamics of soil organic matter degradation. Indeed, aggregate hierarchy occurs with a parallel hierarchy of pores that exist between and within aggregates of varying sizes (Elliott and Coleman 1988). Thus, the smaller pores inside microaggregates (53–250 μm) are more likely to exclude biota and their enzymes than those in larger structures (e.g., macroaggregates 250–2000 μm).

Porosity and microstructure within aggregates change not only with their turnover (i.e., breakdown and reformation), altering activities associated with plant roots and soil fauna (Czarnes et al. 2000; Hussein and Adey 1998), but also with tillage and fertilization management that strongly affects aggregate stability. For instance, Schjønning et al. (2002) found a larger volume of pores >30 μm in an organically managed sandy–loam soil than in an arable one receiving only mineral fertilization. The former also showed a much more complex and tortuous pore system. Pagliai et al. (2004) observed a change in shape and pore size distribution within about a year after compost and manure application. The amended soils resulted in a higher macroporosity than the control, with the highest percentage of elongated pores (belonging to classes 50–500 μm) measured in the livestock manure treatment. On the contrary, Haynes and Naidu (1998) found an increase in total porosity and the relative volume of pores <30 μm after 90 years of farmyard manure application.

Dal Ferro et al. (2012, 2013), integrating micro-CT with mercury intrusion porosimetry techniques, proved that SOC content and its humic fractions have a dual effect on the soil structure, as they favor the formation of both micropores (<5 μm) and macropores (>560 μm).

Although knowledge on the interaction between SOC and the aggregation process is rapidly increasing, the role of humic substances (HS) as binding agents and how exactly their chemical moieties may influence the soil aggregate porosity are still debated. Despite many studies on HS, their detailed nature is not fully understood. HS are operationally defined by a standardized procedure of extraction; however, a complicating factor is their high variability depending on the ecosystem where they are originated (i.e., vegetation, climate, and tillage and fertilization practices). Kelleher et al. (2006), using advanced nuclear magnetic resonance approaches, suggested that the vast majority of operationally defined humic material is a very complex mixture of microbial and plant biopolymers and their degradation products, but not a distinct chemical category. Recent studies have shown that HS are a heterogeneous pool of substances with very different turnover times (Lützow et al. 2007).

For a long time, the formation of recalcitrant HS has been considered as the major pathway for soil organic matter (SOM) stabilization (Piccolo 2002). In fact, the chemical heterogeneity and association with soil minerals make such a macromolecular complex resistant to enzyme attack (Lützow et al. 2007; Marschner et al. 2008). As a consequence, the interaction between HS and soil particles may regulate the C persistence in soils. An improved understanding of these interactions might lead to new strategies for soil C sequestration through HS stabilization. Consistent with previous findings, we expect that pore size distribution can selectively protect specific carbon pools in different aggregate size fractions, influencing soil C sequestration. Moreover, we hypothesize that the strong interaction between SOC and soil structure is due to long-term fertilization practices.

The aim of this study was to investigate the chemical and physical mechanisms of SOC protection associated with specific SOC pools. The samples were collected from a long-term experiment established in the early 1960s in northeastern Italy, where contrasting soils were treated with farmyard manure and mineral fertilization. SOC dependency on chemical and physical protection mechanisms was investigated by aggregate physical fractionation and analyses of pore size distribution, ^{13}C cross-polarization–magic angle spinning nuclear magnetic resonance (CP MAS ^{13}C NMR), and Fourier transform infrared (FTIR) spectroscopies.

2 Material and methods

2.1 The long-term experiment

The long-term trial is located at the Experimental Farm of the University of Padova (Veneto Region, NE Italy). The local climate is sub-humid, with annual rainfall of about 850 mm and yearly average temperature of 12 °C. Reference evapotranspiration (ET_o) is 945 mm with a peak in July (5 mm day^{-1}). ET_o exceeds rainfall from April to September. The site has a shallow water table fluctuating from about 0.5–1.5 m in late winter-early spring to 1–2 m in summer. The experiment began in 1964 in 4-m^2 open lysimeters, 80 cm deep, where three types of soil (hereinafter called clayey (CLY), sand (SND), and peaty (PTY), in relation to their dominant property) (Table 1) were factorially combined with six types of mineral, organic, or mixed fertilization, organized in two randomized blocks (36 lysimeters). The soils were brought from three locations in the Veneto region: clayey soil from the south-western plain, sandy soil from the central coastal area, and peaty soil from the southern plain. The original soil profiles were reconstructed in the lysimeters. The sandy soil (Calcaric Arenosols, Typic Ustipsamments, mixed, mesic—ARPAV, 2005) contains predominantly quartz and feldspar and a significant amount of dolomite (16 %). The clayey soil (Cumulic, Vertic, Endoaquoll fine, mixed, calcareous, mesic—ARPAV, 2005) has a higher amount of smectite/montmorillonite (16 %) than the other soils and a considerable presence of mica (19 %) and dolomite (15 %). The peaty soil (Typic Sulfisaprists, euic, mesic—ARPAV, 2005) is characterized by a higher mica content (25 %), whereas smectite/montmorillonite reaches 12 %. After 40 years of experimental conditions, some original proprieties have changed, as reported in Morari et al. (2008).

Fertilization treatments were as follows: no applications (O), farmyard manure (FYM) (40 t ha^{-1} $year^{-1}$) and mineral fertilizer (Min) (200 kg ha^{-1} $year^{-1}$ N–100 P_2O_5–240 K_2O). The FYM applied almost the same amount of macroelements

as Min, with about 3.5–4 t C ha^{-1} $year^{-1}$. Until 1984, there was a 2-year maize (*Zea mays* L.)—wheat rotation (*Triticum aestivum* L.). Thereafter, a variable rotation was adopted between 1985 and 1992, with various horticultural crops. Since 1993, there has been a 3-year rotation of tomato (*Lycopersicon esculentum* Mill.)–sugarbeet (*Beta vulgaris* L.)–maize, followed by various horticultural crops, maize and sunflower (*Helianthus annuus* L.) from 2003 to 2007. Apart from fertilization, all plots were treated in the same way in terms of rotation and management (tillage, sowing, harvest, etc.). The top 15–20 cm was dug each autumn, and crop residues were removed.

2.2 Soil sampling and fractionation technique

The top soil layer (0–20 cm) was sampled in June 2008. The samples were taken from five different points in the lysimeter and bulked to obtain a sample of about 1 kg. Samples were broken up manually, air-dried, and sieved at 2 mm. To standardize the fractionation procedure and better evidence the relationship between aggregation and organic binding agent in the different soils, we first isolated the large macroaggregates (1000–2000 µm) by dry sieving. More than 50–60 % of the total mass was in the large macroaggregate fraction. No large aggregates were isolated from sandy soil, so all the soil was retained (<2000 µm). Large aggregates (two sub-samples per plot, 36 in total) were then separated into three aggregate size fractions by wet sieving, using an automatic machine oscillator. Briefly, the apparatus produces vertical actions that transmit a 3-cm stroke vertical movement to a stack of interfitting sieves with a mesh of 250 and 53 µm. The sieves, 10 cm in diameter and 5-cm height, were immersed in distilled water inside a beaker (15-cm diameter × 18-cm height). Prior to sieving, the water level was adjusted to prevent water reflux over the edge of the 250-µm sieve during the oscillation. Before sieving, 15 g of sample was immersed on top of the 250-µm sieve for 10 min to allow slaking. After slaking, aggregates were separated by vertical oscillations at a frequency of 50 rpm for 18 min (for a total of 900 oscillations). Macroaggregates (250–2000 µm) and microaggregates (53–250 µm) were then collected from the corresponding sieves, whereas the silt–clay fraction (<53 µm) remaining in the beaker was precipitated by adding 3 mL of 1 N $CaCl_2$. In sandy soil, the silt–clay fraction was not recovered because of its very low amount, and in general, due to the lack of aggregation, we can define macroaggregates (250–2000 µm) and microaggregates (53–250 µm) as medium and fine sand, respectively. All isolated fractions were dried at 60 °C in a forced-air oven.

2.3 Mercury intrusion porosimetry

Mercury intrusion porosimetry (MIP) is commonly accepted as a standard for soil total pore volume and pore size distribution determination (Hajnos et al. 2006; Zaffar and Lu 2015).

Table 1 Physical–chemical characteristics of the 0–30-cm depth at the beginning of the experiment (1964)

Parameters	Clay	Sandy	Peaty
Sand (2 mm–50 µm) (%)	25.0	93.4	38.0
Silt (50–2 µm) (%)	23.0	6.0	13.6
Clay (<2 µm) (%)	52.0	0.6	48.4
pH	7.9 (7.7)	8.1 (7.7)	4.9 (7.2)
Total carbonate (g kg^{-1})	26.0	39.0	0.0
Organic carbon (g kg^{-1})	14.5 (15.7)	1.7 (3.1)	105.0 (89)
Total nitrogen (g kg^{-1})	1.5 (1.5)	0.15	6.7 (6.5)
C/N	10.0 (10.2)	12.0	16.0 (13.6)
Total phosphorus (g kg^{-1})	2.8 (5.6)	0.5 (1.8)	1.1 (3.1)
Available phosphorus (mg kg^{-1})	161.5	26.2	100.4

Values between brackets were measured in 2002

The different aggregate fractions and the starting large macro-aggregates (1000–2000 μm) were analyzed by MIP for total porosity (TP) and pore size distribution (PSD) within the diameter range 0.0035–75 μm. Pores within the range 10–75 μm were analyzed with Thermo Finnigan Pascal 140, while pores within the range 0.0035–10 μm were analyzed with Thermo Finnigan Pascal 240. The pore radius into which Hg was intruded was calculated as a function of pressure using the Young–Laplace equation:

$$r = \frac{2\gamma\cos\theta}{P} \tag{1}$$

where P is the pressure (kPa), r is the radius (μm), λ is the surface tension of mercury (0.47 N m^{-1}), and θ is the contact angle (140°). Pores were labeled with a classification adapted from Cameron and Buchan (2006) as mesopores 30–75 μm (C30–75), micropores 5–30 μm (C5–30), ultramicropores 0.1–5 μm (C0.1–5), cryptopores 0.01–0.1 μm (1) (C0.01–0.1), cryptopores (2) 0.007–0.01 μm (C0.007–0.01), and cryptopores (3) 0.0035–0.007 μm (C0.0035–0.007).

2.4 Soil chemical analysis

Wet-sieved aggregates were analyzed for organic carbon (OC) (g OC kg^{-1} dry soil) by dichromate oxidation (Walkley and Black 1934). The initial fraction 1–2 mm was also analyzed, but OC concentration did not differ from the bulk soil (data not reported).

Humic carbon (HC) was extracted from air-dried soil aggregate fractions (WSA) with 0.5 M NaOH as previously described by Lugato et al. (2010). Here, the term HC is comprehensive of both the humic and fulvic fractions. HC was dialyzed against distilled water and then lyophilized prior to analysis. To perform chemical analysis, the HC extracted from the two replicates was mixed together to form a single sample. In total, 24 HC samples were analyzed (3 soils × 3 treatments × 3 aggregate fractions − 3 silt–clay fractions in sandy soil).

2.5 Fourier transform infrared spectroscopy (FTIR)

FTIR spectra of humic C were recorded with a Bruker TENSOR series FTIR spectrophotometer (Ettlingen, Germany) equipped with an apparatus for diffuse reflectance (Spectra-Tech. Inc., Stamford, CT). The spectra were acquired between 4000 and 400 cm^{-1} by accumulating 64 interferograms at 4-cm^{-1} resolution. A background spectrum using KBr powder (Aldrich Chemical Co. Milwaukee, WI) was recorded prior to collection of each sample spectrum. Analyses of spectral data were performed with Grams/386 spectral software (Galactic Industries, Salem, NH).

2.6 Solid-state ^{13}C nuclear magnetic resonance

Solid-state ^{13}C NMR characterization was performed with a Bruker Avance 400 WB spectrometer equipped for solid-state analysis and operating at 100.61 MHz. A lyophilized sample of 100 mg was packed into a 4-mm zirconia rotor with Kel-F caps and spun at a speed of 12.5 kHz. Further details were described in Simonetti et al. (2012).

The spectra were divided into five regions according to Helfrich et al. (2006): (i) alkyl C (0–35 ppm) of lipids, fatty acids, and plant aliphatic polymers; (ii) O,N-alkyl C (35–90 ppm) deriving primarily not only from polysaccharides but also from proteins; (iii) anomeric C (90–108 ppm) of cellulose and hemicellulose; (iv) aromatic or aryl C (108–158 ppm); and (v) carbonyl C (158–182 ppm) from esters, carboxyl groups, and amide carbonyls (Chen and Chiu 2003; Helfrich et al. 2006). Integration of the peaks within each of the chemical shift regions allowed the evaluation of the relative C contents expressed as percentages of the total area.

2.7 Statistical analysis

Soil porosity, SOC, and HC were analyzed with ANOVA, and significantly different means were estimated by using the Student–Newman Keuls test (StatSoft Inc 2004). The ^{13}C NMR characterizations of SOC extracted from the two replicates were mixed together to form a single sample. In total, 24 HS samples were analyzed (3 soils × 3 treatments × 3 aggregate fractions − 3 silt–clay fractions in sandy soil). To clarify the structure of these interdependences, we performed a joint principal component analysis (PCA) of our data on the 12 variables: (i) five porosity classes (relative frequency values of mesopores, ultramicropores, and cryptopores (1), (2), (3)); (ii) the TP percentage; (iii) OC content; and (iv) four integrated peak areas of the main ^{13}C chemical shift: carbonyl C, aryl C, anomeric C, O,N-alkyl C. The PCA variables were selected on the basis of the Kaiser–Meyer–Olkin (KMO) test as a measure of sampling adequacy, obtaining a KMO value of 0.60. Data were submitted to the principal component (PC) analysis; rotated orthogonal components (varimax normalized method of rotation) were extracted, and the relative scores were determined. Only PCs with eigenvalues >1 were considered for the discussion.

3 Results

3.1 Physical analysis

Porosity varied in the aggregate fractions, while no statistical difference was due to the treatments. Higher total porosity (TP) (Fig. 1) was measured in microaggregate (53–250 μm) and silt–clay (<53 μm) fractions than in macro (250–2000 μm) ($p < 0.01$) and large (1000–2000 μm) aggregates.

Fig. 1 Total porosity (%) for the different aggregate size fractions and large aggregates (1000–2000 μm)
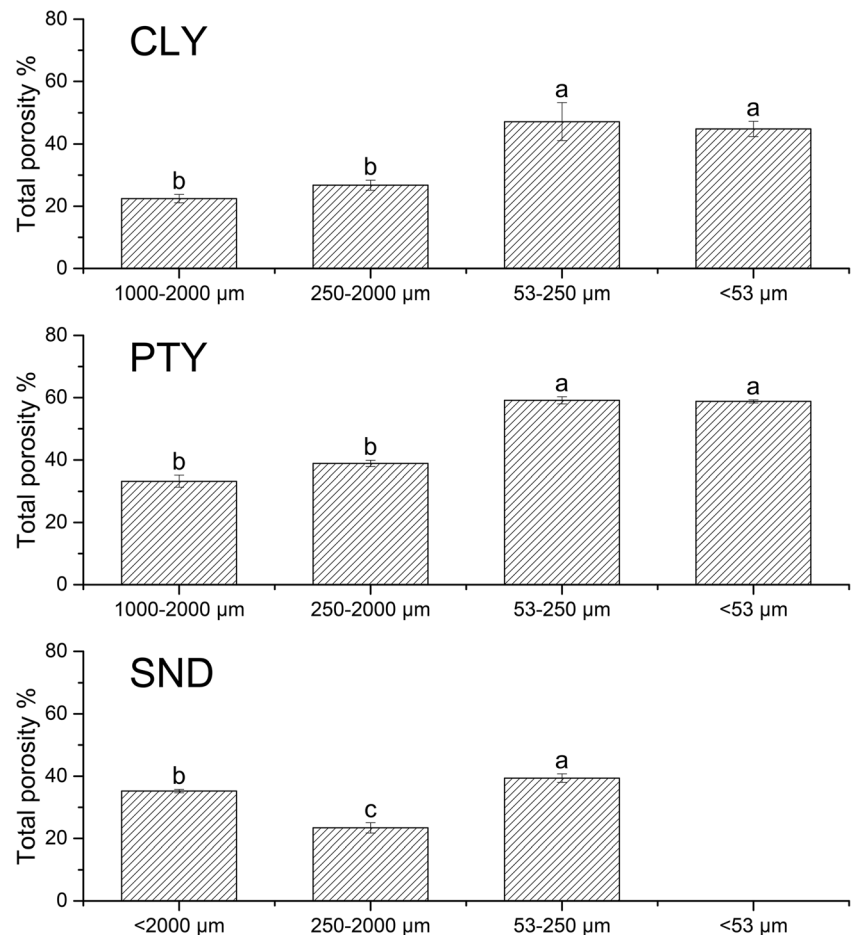
In particular, TP was 59 % for micro and silt–clay fractions in PTY and 47 and 44 %, respectively, in CLY. Low TP was instead measured in SND with 39 % in medium sand and 23 % in fine sand fractions, while the sand (<2000 μm) was, as expected, in the middle (35 %).

Pore size distribution (PSD) changed significantly ($p < 0.01$) in CLY according to the aggregate fractions (Figs. 2 and 3) but not with treatments. However, long-term FYM amendment led to an apparent increase of volume in porosity classes <5 μm (data not shown). Higher C30–75 values were observed in the macro (250–2000 μm) and micro (53–250 μm) fractions (0.07 and 0.09 cm^3 cm^{-3}) than in the silt–clay. On the contrary, micropore class (C5–30) exhibited higher volumes in microaggregate (0.30 cm^3 cm^{-3}) than in silt–clay (<53 μm) and macroaggregate (0.07 cm^3 cm^{-3}) fractions. Ultramicropores (C0.1–5) were higher in silt–clay (0.20 cm^3 cm^{-3}) than the other two classes, while cryptopores (from 1 to 3) had similar distribution with higher values in macroaggregate fraction (Figs. 2 and 3).

As observed for clayey soil, the porosity in PTY was not influenced by treatments even if FYM amendment led to an apparent increase of cryptopore (<C0.01–0.1) volumes. PSD was significantly different ($p < 0.05$) between aggregate fractions. Mesopores (C30–75) and micropores (C5–30) were mostly distributed in microaggregate (0.12 and 0.31 cm^3 cm^{-3}) with respect to macroaggregate and silt–clay fractions. Ultramicropore (C0.1–5) class was the most frequent in silt–clay (<53 μm) (0.38 cm^3 cm^{-3}), corresponding to 60 % of TP. Cryptopore (1), (2), and (3) classes showed a similar distribution to that observed for CLY soil. Macroaggregates had the highest values ($p < 0.01$), while no statistical differences were observed in silt–clay.

The porosity in SND soil was considerably influenced by treatments. Indeed, mesopore (C30–75) distribution was statistically ($p < 0.01$) higher in Min fertilization (0.20 cm^3 cm^{-3}) than in FYM (0.13 cm^3 cm^{-3}) and the control (0.15 cm^3 cm^{-3}). Mesopores (C30–75), micropores (C5–30), and cryptopores (1) were more frequent in microaggregates (53–250 μm) (Figs. 2 and 3). The other classes (C0.1–5, cryptopores (2) (3)) did not exhibit significant differences between the fractions.

3.2 Chemical analysis

The silt–clay fraction was significantly depleted in OC content ($p < 0.05$) with respect to microaggregate (53–250 μm) and

Fig. 2 Quantitative (q) (cm³/cm³) pore size distribution (PSD) in the range 0.0035–75 μm for the different aggregate size fractions. Within each porosity class, histograms having the *same letter* are not statistically different at $p < 0.05$. *Bars* represent the standard error
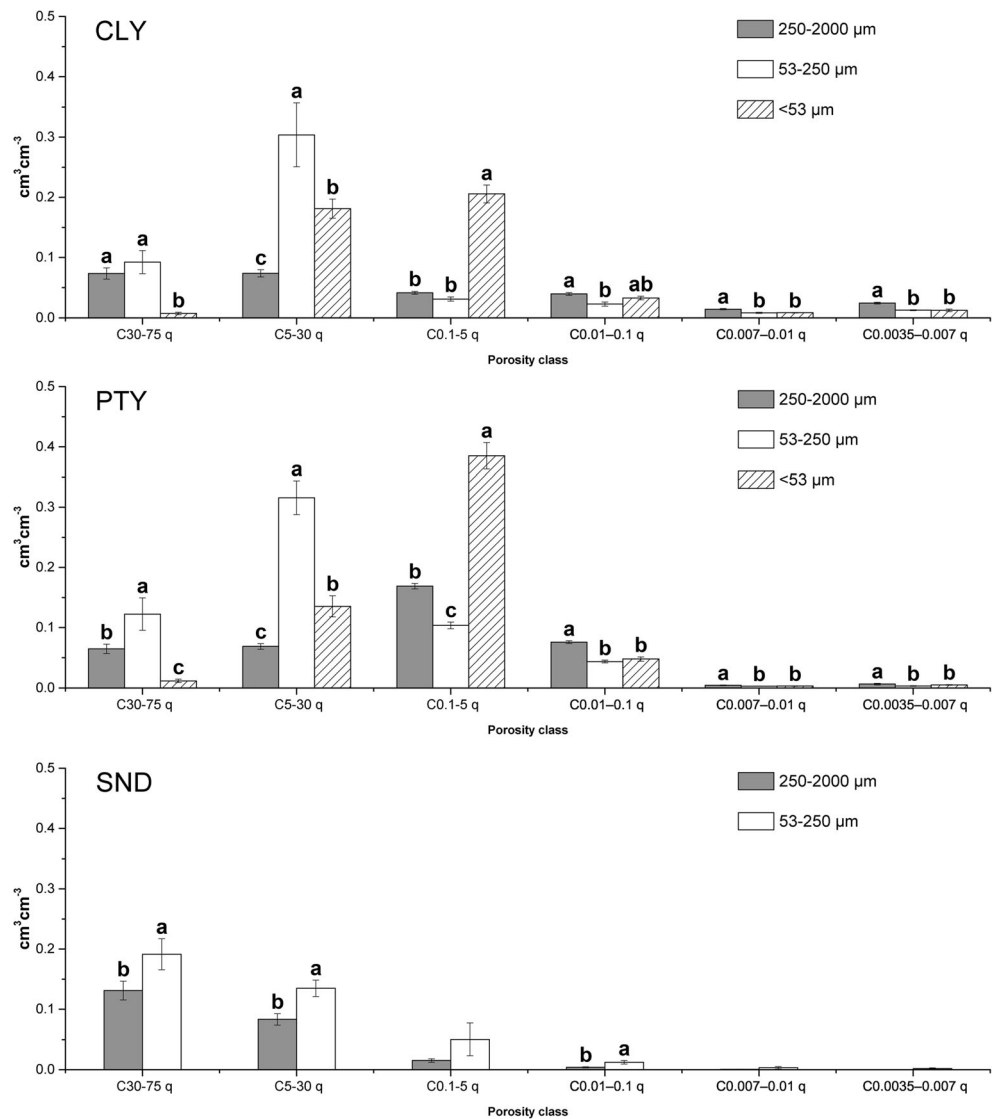
macroaggregates (250–2000 μm) of CLY and PTY soils (Table 2). Microaggregates and macroaggregates exhibited similar values between treatments, apart from FYM associated with CLY soil, where SOC showed the highest values for both macroaggregate and microaggregate fractions (21.75 and 27.02 g C kg⁻¹ aggregate, respectively). Similar results were observed for PTY soil (Table 2). Conversely, the OC concentration in SND soil did not show significant differences in either aggregate fractions or between treatments; however, the FYM amendment gave a higher OC concentration ($p < 0.05$) than the control and Min treatments. The determination of HC can provide an estimate of the effects of different treatments on SOC humification processes. In CLY and PTY soils, the HC concentration was considerably influenced by long-term FYM input compared to the control and Min fertilization (Table 2). With respect to the aggregate fractionations, the HC concentration in microaggregate and macroaggregate was not different in either soil, whereas it differed ($p < 0.05$) in

silt–clay. Instead, no statistical differences were found in SND soil.

The HC/OC ratio did not reveal a clear pattern in relation to soil aggregation, since no significant differences were observed between CLY and PTY soils. However, higher values were found in macroaggregates as affected by FYM and Min treatments in the CLY and PTY soils, respectively.

3.3 Fourier transform infrared spectra (FTIR)

The HC spectra from different soil aggregate fractions (Fig. 4) showed the spectral pattern of HS described in the literature (Mafra et al. 2007; Francioso et al. 2007; Mao et al. 2007; Francioso et al. 2009; Simonetti et al. 2012). Humic C spectra were characterized by a broad band around 3500–3300 cm⁻¹ (OH stretch of different groups), a shoulder at around 3100–3040 cm⁻¹ (NH₃⁺ stretch and C=CH stretch vibrations), peaks at around 2960 and 2870 cm⁻¹ and 2930 and 2940 cm⁻¹ (CH₃

Fig. 3 Relative (%) pore size distribution (PSD) in the range 0.0035–75 μm for the different aggregate size fractions. Within each porosity class, histograms having the *same letter* are not statistically different at *p* < 0.05. *Bars* represent the standard error
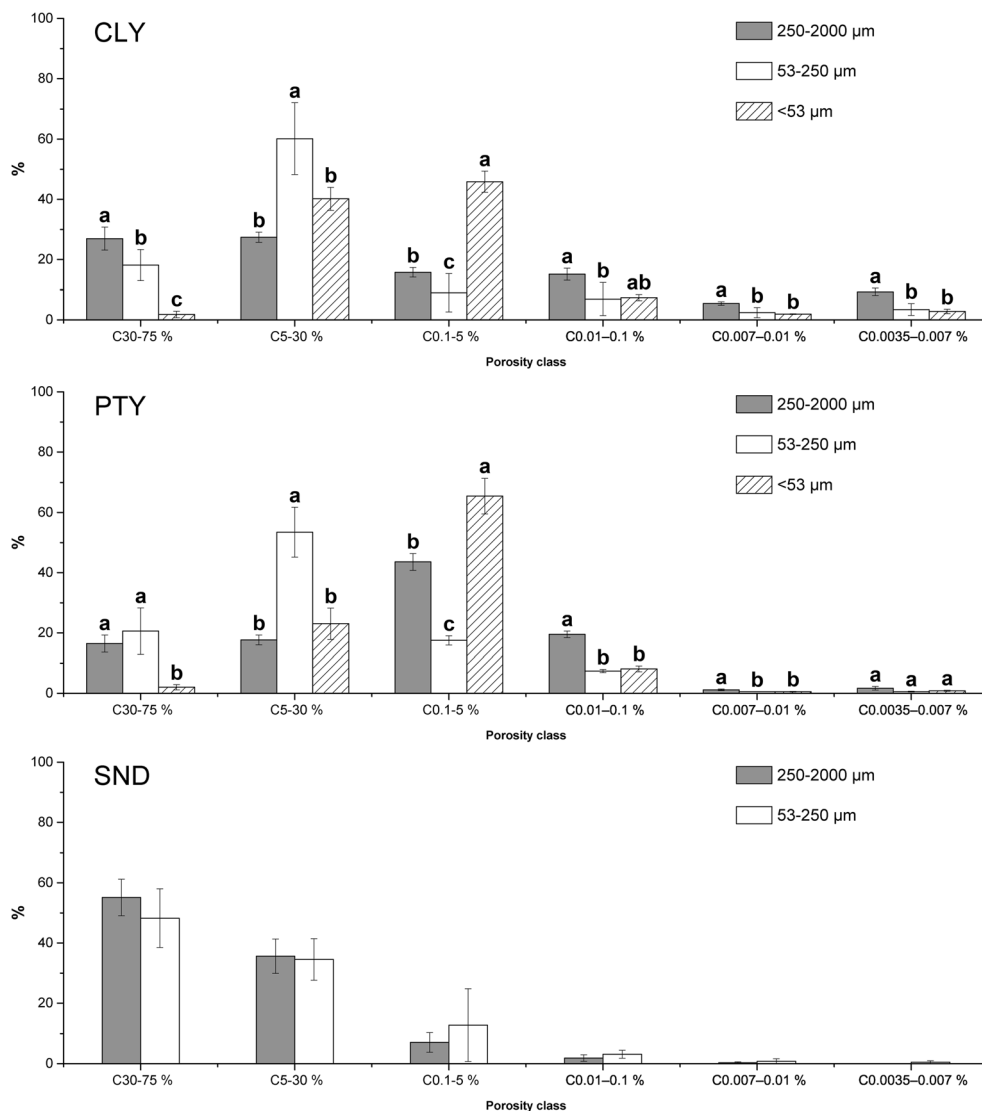
and CH$_2$ stretch of aliphatic chains, respectively), a broad band at 2600–2500 cm^{-1} (OH stretch in dimeric acids), a strong band at around 1720–1700 cm^{-1} (C=O stretch of carboxylic acids), an intense band at around 1650 cm^{-1} (amide I, C=C stretch vibration in aromatic rings and C=O stretch in ketone), a medium peak at around 1560 cm^{-1} (amide II, aromatic rings, asymmetric stretch of COO$^-$), a weak peak at around 1450 cm^{-1} (CH$_3$ asymmetrical bending and CH$_2$ scissoring vibrations, symmetric stretch of COO$^-$), a variable intensity peak between 1230 and 1250 cm^{-1} (amide III, C–O stretch of aromatic rings and carboxylic acids), a strong peak between 1100 and 1030 cm^{-1}, and a minor absorption peak at 820 cm^{-1} (C–O stretch of cellulose and other β-anomers and β-glycosides).

Humic C from aggregate fraction spectra of untreated CLY soil (Fig. 4) was very similar. Conversely, after 44 years of Min fertilization, the HC spectra showed some structural modification between aggregates in terms of relative intensity changes of carbonyl (1712 cm^{-1}) and C–O groups (1234 cm^{-1}). Moreover, C–O group shifted toward lower frequencies in 53–250- and <53-μm aggregate fractions with respect to 250–2000-μm ones. This might imply an involvement of C–O group in carboxylic acids rather than C–OH in phenols (Rao 1963). Likewise in FYM amendment (Fig. 4), the HC spectra exhibited the principal variations in the carbonyl (1709 cm^{-1}) and C–O groups (1218 cm^{-1}) that seem to be the most interesting vibrations as regard aggregate size. The relative intensity of these bands gradually increased in the micro (53–250 μm) and silt–clay (<53 μm) fractions. A shift to higher frequencies of the C–O group was observed in the 53–250-μm (+16 cm^{-1}) and <53-μm fractions (+22 cm^{-1}) suggesting the presence of C–O group in the phenolic structure (Rao 1963). Min and FYM fertilization had a positive effect on the distribution of some functional groups of HC

Table 2 Organic carbon (g/kg), humic carbon (g/kg), and HC/OC ratio for the different treatments in CLY, PTY, and SND soils

Fraction (µm)	CLY								
	OC (g/kg)			HC (g/kg)			HC/OC		
	0	MIN	FYM	0	MIN	FYM	0	MIN	FYM
250–2000	15.22 cd	16.22 c	21.75 b	5.72 b	6.52 b	11.94 a	0.38 b	0.40 b	0.56 a
53–250	14.02 cd	14.65 cd	27.02 a	5.35 b	5.98 b	12.99 a	0.38 b	0.41 b	0.48 ab
<53	12.13 d	9.61 e	15.05 cd	4.18 b	4.71 b	6.26 b	0.35 b	0.49 ab	0.42 b
	PTY								
	OC (g/kg)			HC (g/kg)			HC/OC		
	0	MIN	FYM	0	MIN	FYM	0	MIN	FYM
250–2000	66.94 abc	58.66 abc	91.94 a	32.68 abc	34.50 abc	44.02 a	0.49 ab	0.59 a	0.48 ab
53–250	65.04 abc	59.89 abc	85.89 ab	36.04 abc	31.69 abc	42.72 ab	0.55 ab	0.53 ab	0.50 ab
<53	42.22 bc	37.95 c	45.14 bc	15.06 c	16.66 c	20.31 bc	0.36 c	0.44 bc	0.45 bc
	SND								
	OC (g/kg)			HC (g/kg)			HC/OC		
	0	MIN	FYM	0	MIN	FYM	0	MIN	FYM
250–2000	2.17	1.43	2.83	2.22	1.80	2.78	1.04	1.23	1.05
53–250	1.59	1.20	2.48	1.54	1.33	2.22	0.97	1.10	1.00

Values with different letters are significantly different at $p = 0.05$

from CLY soil aggregate sizes. More acid groups were dominant with Min fertilization, while phenolic structure increased with FYM amendment.

Humic C spectra of untreated PTY soil aggregate sizes (Fig. 4) showed variations in the relative intensity of the peaks from 2930 to 2880 cm^{-1} (aliphatic groups), 1550 cm^{-1} (amide II, aromatic rings), 1223 cm^{-1} (C–O groups), and 1040 cm^{-1} (carbohydrates). The aliphatic region seems to be more intense in the 250–2000-µm fractions, whilst the C–O and carbohydrate groups considerably increased in the microaggregate (53–250 µm) fraction. Fertilization with Min (Fig. 4) did not lead to substantial modification of functional groups between the HC spectra of macro (250–2000 µm) and micro (53–250 µm) fractions. Conversely, the silt–clay fraction showed an enhancement in relative intensities of the bands at 1710 cm^{-1} (carbonyl group), 1233 cm^{-1} (C–O group), and 1048 cm^{-1} (carbohydrates). After 44 years of FYM amendment (Fig. 4), no significant difference was observed among functional groups attributable to treatment.

Humic C spectra from medium and fine particles of untreated SND soil did not differ (Fig. 3). Min fertilization did not change the pattern of HC from macro (250–2000 µm) size fraction with respect to the untreated one; instead, micro (53–250 µm) fraction differed by the lack of a broad band at 2655 cm^{-1} (OH stretch in dimeric acids). FYM did not seem to cause significant modification between macroaggregate and microaggregate (53–250 µm) fractions. However, the FYM amendment seemed to increase the relative intensity of the band at 1650 cm^{-1} (amide I, C=O in ketone) with respect to untreated and Min fertilization.

3.4 Solid-state ^{13}C nuclear magnetic resonance

NMR spectra of HC from the untreated CLY aggregate size fractions were characterized by different percentage distributions of ^{13}C between fractions (Table 3; Fig. 5). Humic C from macroaggregate of CLY soil showed the highest content of O,N-alkyl/methoxyl groups (54 %, Table 3; Fig. 5), probably derived from root residues (hemicellulose and cellulose), and a smaller proportion of aromatic C (aryl C) (5.1 %, Table 3; Fig. 4). In contrast, HC from the microaggregate (53–250 µm) fraction exhibited a high level of aromatic C (~6 %, Table 3; Fig. 4) and carbonyl C (~20 %, Table 3; Fig. 4). Alkyl and anomeric C were prevalent in HC from silt–clay (<53 µm). Mineral fertilization caused a decrease in O,N-alkyl C content from macro (54 %) to silt–clay (50 %) size fractions (Table 3; Fig. 4), whereas the alkyl C content was variable. Conversely, HC from microaggregate (53–250 µm) fraction showed the highest O,N-alkyl and alkyl C content, suggesting that root residues were not so extensively decomposed in this fraction. The low aromatic C content also found in this fraction might also support this evidence. Humic C from silt–clay (<53 µm) fraction was markedly characterized by higher amounts of aromatic (~6 %) and carbonyl C (~21 %) than in the other treatments.

Fig. 4 Diffuse reflectance
infrared Fourier transform
(DRIFT) spectra of humic carbon
(HC) extracted from different
aggregate size fractions of CLY,
PTY, and SND soils:
macroaggregate (250–2000 μm),
microaggregate (53–250 μm),
and silt–clay (<53 μm)
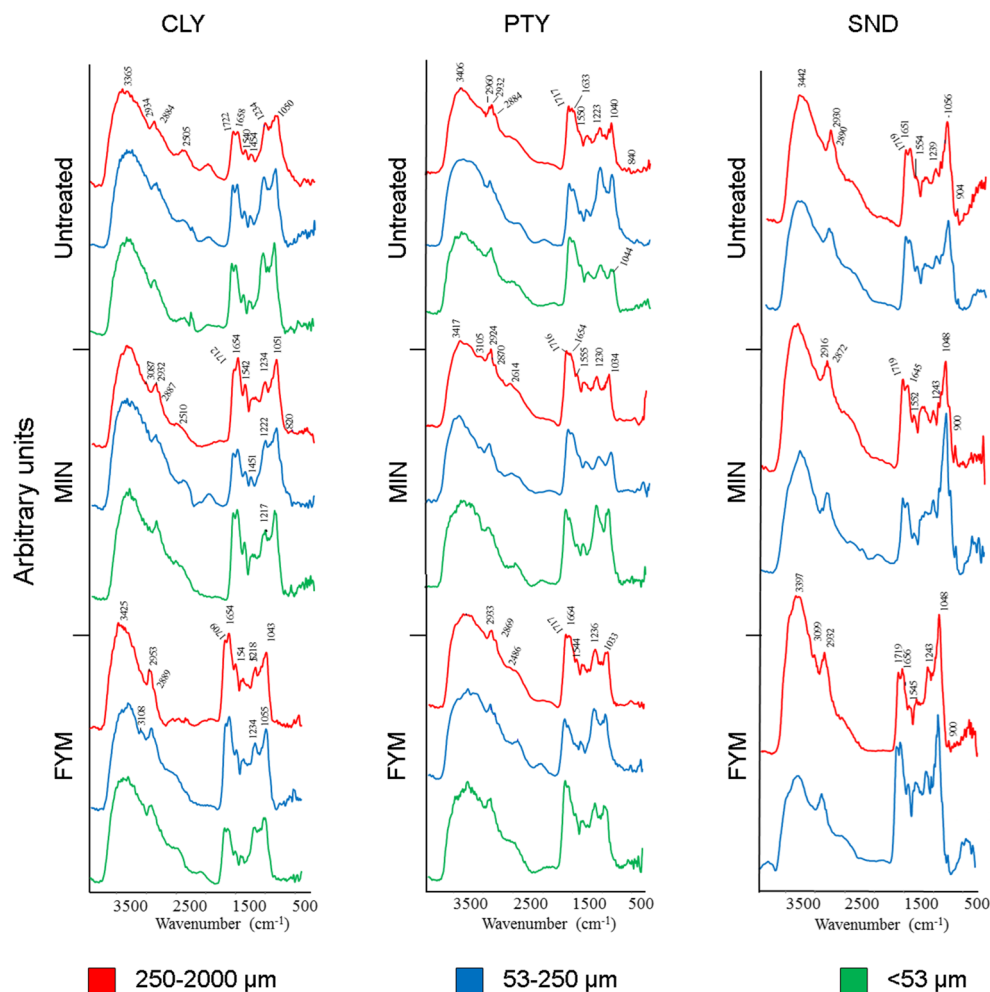
FYM amendment caused a decrease in O,N-alkyl C and alkyl C in microaggregate (53–250 μm) and silt–clay fractions, whereas the anomeric C content did not seem to be affected. However, it decreased with respect to the other treatments. An increase in aryl C (~12 %), carbonyl C (~20 %) and the presence of phenolic compounds (150 ppm, spectrum not shown) were instead observed in macroaggregate (250–2000 μm) fraction.

In the HC spectrum from untreated PTY soil, a progressive decrease was observed in proportion of alkyl C and O–N alkyl C between aggregate fractions (Table 3; Fig. 4). In contrast, the proportion of aromatic C increased from macro (250–2000 μm) to silt–clay (<53 μm) size fractions. Min fertilization led to a progressive increase in O,N alkyl C content from macroaggregate (250–2000 μm) to silt–clay fractions, while alkyl C was more accumulated in the microaggregate fraction. In addition, the alkyl C/O and N alkyl C ratio tended toward 1 in microaggregate (53–250) fraction.

In HC from silt–clay (<53 μm) fraction, a high proportion of O,N alkyl C (~43 %) and a low aromatic C content (~17 %) were observed (Table 3; Fig. 4).

FYM amendment gave an HC similar to those of untreated soil (Fig. 4). However, the amount of alkyl C and O,N alkyl C progressively decreased from macroaggregate to silt–clay fractions, while the amount of aromatic C and carbonyl C progressively increased (Table 3; Fig. 4). The presence of phenols (~150 ppm, spectrum not shown) was only found in the macroaggregate and microaggregate fractions, while no resonance was observed in untreated fractions.

Humic C from aggregate fractions of untreated SND soil was characterized by the lowest percentage of alkyl C (Table 3; Fig. 4) with respect to other soil fractions. N,O alkyl C and anomeric C in medium (~67 and 12 %, respectively) and fine (61 and 12 %, respectively) fractions did not differ, but their content was unexpectedly high. The amount of aromatic and carbonyl C increased in medium sand (53–250 μm). Mineral fertilization led to an accumulation of alkyl C and N,O alkyl C in medium sand fraction, whilst anomeric C (17 %), aromatic C (~10 %), and carbonyl C (~7 %) increased in fine sand (53–250 μm) fraction. FYM amendment led to a magnification of alkyl C, aromatic C, and carbonyl C in both size fractions compared to other treatments (Table 3; Fig. 4).

Table 3 CP MAS ^{13}C NMR relative peak area (%) for humic C isolated from different aggregate size fractions of clay, peaty, and sandy soils fertilized consecutively over 40 years with mineral (Min) and manure (FYM)

|	Alkyl C 0–35 ppm	O,N alkyl C 35–90 ppm	Anomeric C 90–108 ppm	Aryl C 108–158 ppm	Carbonyl C 158–182 ppm
Clay (CLY) (μm)					
Untreated					
2000–250	16.5	55.0	4.9	5.1	18.4
53–250	16.5	52.9	4.6	6.4	19.6
<53	20.3	50.2	5.6	5.4	18.5
Min (μm)					
2000–250	13.6	54.0	5.5	5.6	18.3
53–250	19.9	54.5	4.3	4.3	17.1
<53	16.6	50.1	5.7	6.3	21.3
FYM (μm)					
2000–250	20.0	53.9	3.6	6.9	15.5
53–250	11.8	51.6	3.8	12.1	20.6
<53	19.6	51.6	3.5	6.7	18.5
Peaty (PTY)					
Untreated (μm)					
2000–250	20.9	37.3	1.7	24.2	15.8
53–250	17.3	31.5	2.5	30.4	18.2
<53	11.3	25.3	1.6	35.3	26.4
Min (μm)					
2000–250	17.3	29.2	3.2	33.3	17.0
53–250	27.8	35.1	1.6	21.2	14.2
<53	19.6	42.6	2.5	16.8	18.3
FYM (μm)					
2000–250	15.3	31.8	3.4	32.9	16.5
53–250	15.1	26.0	4.3	37.9	16.6
<53	11.6	24.6	nd	38.5	25.2
Sandy (SND)					
Untreated (μm)					
2000–250	6.5	67.2	12.0	4.4	10.1
53–250	8.7	61.0	12.1	7.1	11.2
Min (μm)					
2000–250	9.4	69.0	11.4	3.8	6.5
53–250	2.3	63.3	17.0	10.3	7.2
FYM (μm)					
2000–250	14.4	56.3	6.1	10.2	13.0
53–250	17.0	50.4	7.3	12.0	14.0

N,O alkyl C and anomeric C tended to decrease with respect to other treatments.

3.5 Correlation and principal component analysis analyses

In mineral soils, significant relationships were found between pore classes and chemical parameters (Table 4). The C30–75 pores were positively correlated ($p < 0.05$) with OC, HC/OC ratio, O,N-alkyl C, and anomeric C and negatively with OC, alkyl C, and carbonyl C. The C0.1–5 pores had a positive correlation with carbonyl C and alkyl C and a negative one with O,N-alkyl C ($r = -0.64$). Cryptopores (1), (2), and (3) showed positive correlations with OC ($r = 0.80$, on average) and carbonyl C, while they were negatively correlated with HC/OC ratio ($r = -0.65$, on average). On the contrary, the C30–75 pore size class in the PTY was positively correlated ($p < 0.05$) with OC and HC/OC ratio and negatively with carbonyl C content. The C0.1–5 pores were positively correlated ($p < 0.05$) with carbonyl C and negatively with OC, HC/OC ratio ($r = -0.60$ and $r = -0.67$, respectively), and alkyl C ($r = -53$).

Fig. 5 Cross-polarization–magic angle spinning (CP MAS) ^{13}C nuclear magnetic resonance (NMR) spectra of humic carbon (HC) extracted from different aggregate size fractions of CLY, PTY, and SND soils: macroaggregate (250–2000 μm), microaggregate (53–250 μm), and silt–clay (<53 μm)

■ 250-2000 μm   ■ 53-250 μm   ■ <53 μm
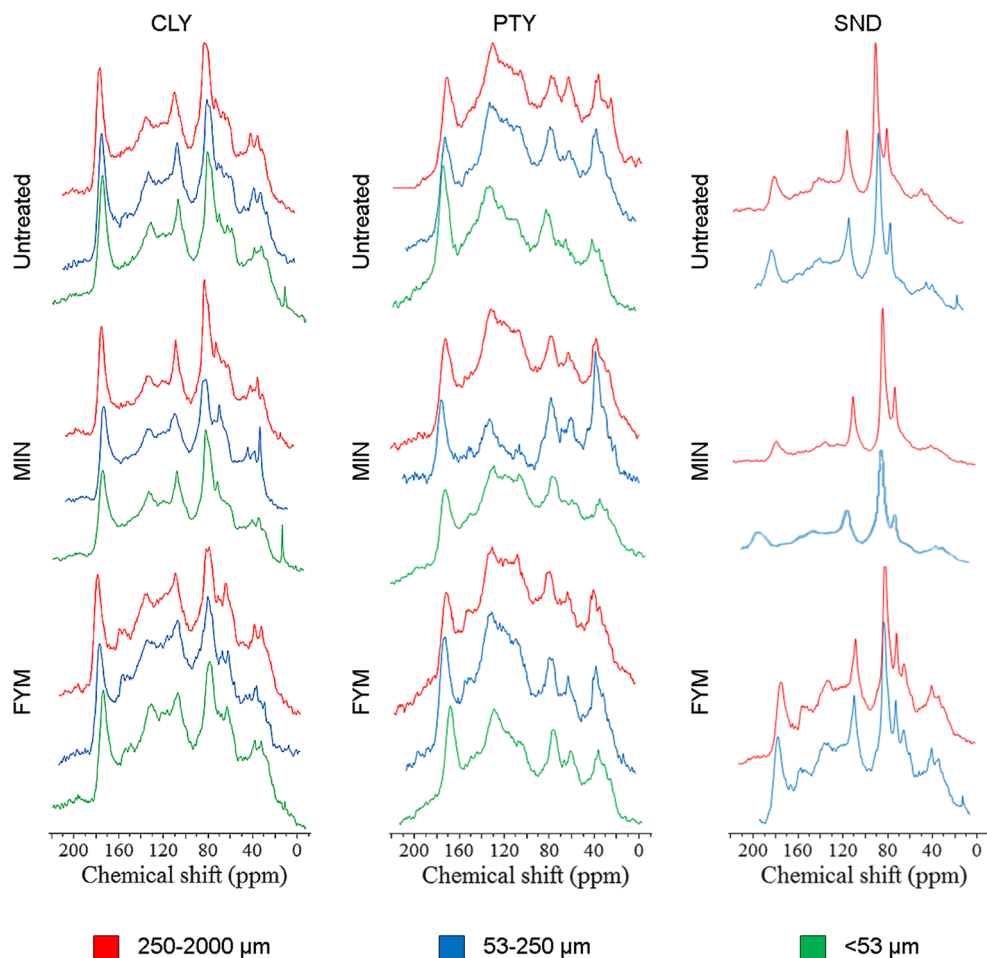
Multivariate analysis was conducted only for the mineral soils (CLY and SND) since potential physical mechanisms of SOC protection in PTY were masked by the high inherent SOC. Application of PCA to mineral soils allowed three PCs to be extracted, explaining 87 % of the variability (Table 5; Fig. 6). PC1 explained 59 % of the variance and was inversely correlated (factor loadings >0.7) with OC content and cryptopores (1), (2), and (3). PC2 explained 19 % of the variance and was correlated with C0.1–5 pores, TP, and carbonyl C, while it was inversely correlated with C30–75 pores, O,N alkyl C functional group, and HC/OC ratio. PC3 explained 10 % and was correlated with aryl C content. The plot of variables and cases, according to PC1 and PC2 and reported in Fig. 6, identified three clusters. The first one was represented by CLY macroaggregate fraction, which was mainly isolated by cryptopores (1), (2), and (3) and OC content. The second cluster showed CLY 53–250 and <53 μm mainly isolated by carbonyl C, C0.1–5 pores, and TP. Finally, the third cluster isolated the medium and fine fraction of SND soil and O,N-alkyl C, anomeric C, C30–75 pores, and HC/OC ratio.

4 Discussion

Soil porosity distribution strongly affects SOC dynamics, in some cases promoting a faster SOC turnover, but in others enhancing its protection (or stabilization) as a result of pore space inaccessibility to microorganisms and enzymes. This occurs in the microporosity to cryptoporosity domain, where organic matter might also interact with clay minerals by intercalation or adsorption (Lützow et al. 2006). Strong et al. (2004), studying the spatial location of C composition in the soil pore system, found a strong correlation ($r = 0.92$) between total C and pore volume <1.2 μm. Conversely, they observed a negative correlation ($r = -0.35$) for total C and pore volume in the range 15–60 μm. Other recent findings corroborated those previously reported: for example, Pituello et al. (2016) extensively studied the long-term effect of residue incorporation on the soil pore structure (0.25 nm–2.5 mm) of three contrasting soils and highlighted a positive correlation between nanopores (10–50 μm) and OC content that was likely due to an OC-mediated stimulus to particle aggregation, while larger pores (30–75) were contemporarily reduced. These

Table 4 Correlation matrix of selected soil parameters

	OC (g/ka)	HC (g/kg)	HC/OC	Carbonyl C	Aryl C	Anomeric C	O,N alkyl C	Alkyl C
Mineral soil (CLY-SND)								
c75–30 %	*0.70*	*0.58*	*0.88*	*0.90*	0.09	*0.79*	*0.85*	*0.79*
c30–5 %	0.19	0.08	−0.35	0.33	−0.17	−0.27	−0.20	0.25
c5–0.1 %	0.23	0.16	−0.44	*0.53*	0.03	−0.43	*0.64*	*0.55*
Cryptopores (1), (2), (3) %	*0.80*	*0.80*	*0.65*	*0.59*	−0.02	*0.61*	−0.50	0.44
Total porosity (%)	0.12	−0.05	−0.43	0.40	−0.03	−0.14	−0.43	0.27
c75–30 q	*0.62*	*0.55*	*0.74*	*0.80*	0.24	*0.83*	*0.69*	*0.80*
c30–5 q	0.25	0.11	−0.46	0.42	−0.13	−0.29	−0.34	0.32
c5–0.1 q	0.14	0.04	−0.42	*0.50*	−0.03	−0.35	*0.59*	*0.51*
Cryptopores (1), (2), (3) q	*0.78*	*0.68*	*0.84*	*0.79*	−0.16	*0.70*	*0.68*	*0.60*
Peaty (PTY)								
c75–30 %	*0.66*	*0.79*	*0.72*	*0.71*	−0.11	0.40	0.18	0.45
c30–5 %	0.17	0.24	0.26	−0.26	−0.02	0.11	−0.13	0.38
c5–0.1 %	*0.60*	*0.72*	*0.67*	*0.68*	0.05	−0.38	−0.02	*0.53*
Cryptopores (1), (2), (3) %	0.41	0.43	0.33	−0.34	0.05	0.28	0.12	0.00
Total porosity (%)	−0.37	−0.42	−0.39	0.37	0.00	−0.28	−0.16	−0.05
c75–30 q	*0.57*	*0.70*	*0.65*	*0.64*	−0.11	0.38	0.12	0.45
c30–5 q	0.16	0.21	0.19	−0.28	−0.09	0.18	−0.06	0.40
c5–0.1 q	*0.72*	*0.85*	*0.77*	*0.84*	0.12	*0.57*	−0.14	*0.57*
Cryptopores (1), (2), (3) q	0.42	0.40	0.22	−0.30	0.05	0.25	0.14	−0.05

Values in italics are significantly different at $p = 0.05$

Table 5 Factor loadings (varimax normalized) calculated for selected soil parameters

Factor loadings (varimax normalized)

Extraction: principal components

|	Factor 1	Factor 2	Factor 3
c75–30 %	*−0.91*	−0.36	0.09
c5–0.1 %	*0.72*	0.07	0.14
c0.1–0.01 %	0.17	*0.96*	0.05
c0.01–0.007 %	0.13	*0.97*	0.03
c0.007–0.0035 %	0.09	*0.97*	−0.07
Total porosity (%)	*0.75*	−0.39	−0.14
OC (g/ka)	0.45	*0.80*	−0.04
HC/OC	*−0.74*	−0.57	0.28
Carbonyl C	*0.81*	0.52	−0.04
Aryl C	0.02	−0.03	*0.98*
Anomeric C	−0.64	−0.61	0.04
O,N alkyl C	*−0.84*	−0.39	−0.30
% Total variance	58.6	19.0	9.8

Marked loadings are >0.7

Factor loadings range between −1 and 1. Loadings close to −1 or 1 indicate that the factor strongly affects the variable. Loadings close to zero indicate that the factor has a weak affect on the variable. However, there is not a significance related to factor loadings and the value of 0.7 is generally accepted as a cut-off criteria

results are consistent with our data on mineral soils (SND and CLY), since strong correlations were found between OC, cryptopores (C0.1–5) and mesopores (C30–75), 0.80 and −0.70, respectively. Conversely, PTY soil showed a positive correlation between mesopores and OC content, most likely because of the direct contribution of SOC internal porosity to bulk soil porosity (Zaffar and Lu 2015).

SOC protection from decomposition is enhanced in small microaggregates particularly rich in pores <0.2-μm diameter. Kaiser and Guggenberger (2003) suggested that the clogging of very small micropores (<2 nm) caused by the SOC sorption could be an additional mechanism against chemical and biological attack. The same authors also found a close relation between large pores and SOC from plant residues enriched in labile materials. Other studies demonstrated that organic matter increased the number of larger pores of soils and favored the formation and stabilization of biogenic macropores (Pagliai et al. 2004; Oorts et al. 2007; Grosbellet et al. 2011; Zaffar and Lu 2015). Among labile components of SOM, the polysaccharides stabilize the soil by binding small particles into microaggregates and then into macroaggregates (Six et al. 2004). Our results confirmed the existence of a close correlation between mesopores and anomeric C (cellulose and hemicellulose) and O,N alkyl C deriving primarily from polysaccharides and proteins (Table 4).

On the contrary, micropores, abundant in microaggregates and silt–clay fractions (Figs. 2 and 3), were correlated with

Fig. 6 Factor loadings for the 12 variables used in principal component analysis (PCA) and cases
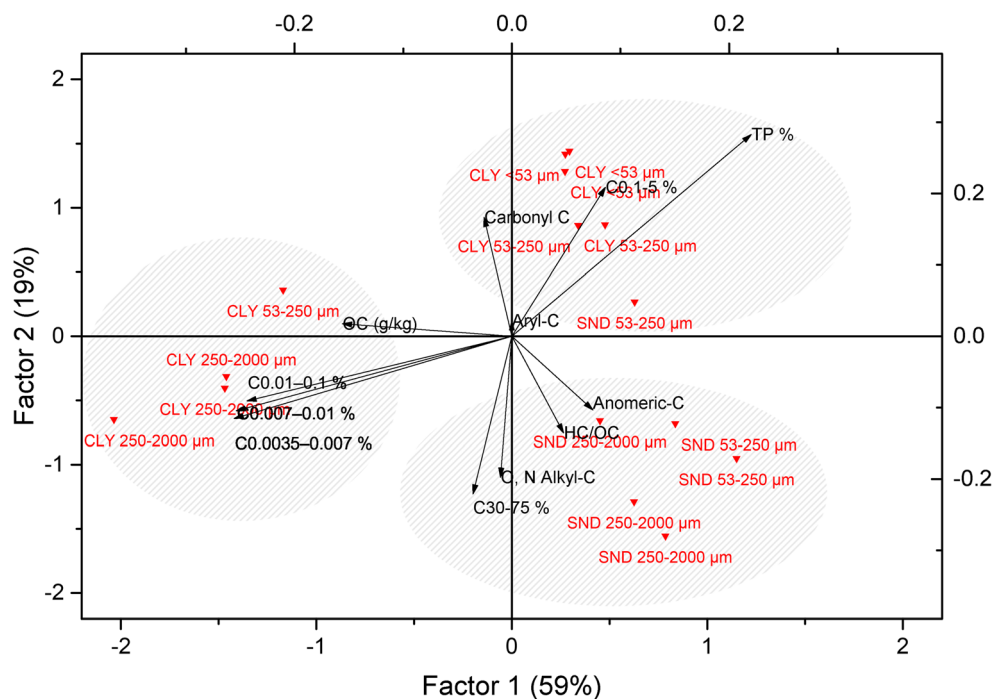
carbonyl C and alkyl C (compounds represented by fats and waxes deriving from plants, fungi, and bacteria), the latter being considered to be resistant to degradation due to its apolar nature (Derenne and Largeau 2001). In particular, the semicrystalline nature of polymethylenic chains might justify the recalcitrance of alkyl C (Hu et al. 2000). Mechanisms of physical preservation, occlusion within aggregates and adsorption onto minerals (Six et al. 2000), could play a major role in carbonyl and alkyl C stabilization. Carbonyl C could form organomineral associations through, e.g., ligand exchange and polyvalent cation bridges, while alkyl C favors weak interactions, such as hydrophobic interactions including van der Waals forces and H-bonding (Vermeer and Koopal 1998; Vermeer et al. 1998). Therefore, molecules sorbed to mineral surfaces cannot be utilized by microorganisms (Chenu and Stotzky 2002) resulting in more resistance to enzyme attack (Theng 2007; Khanna et al. 1998).

Lastly, aryl C is not correlated with specific pore class, evidencing potential mechanisms of biochemical recalcitrance. Indeed, aromatic compounds such as tannins and polyphenols could form complexes with proteins and inhibit the activity of soil enzymes (Freeman et al. 2004).

As confirmed by PCA analyses (Fig. 6), possible mechanisms involved in SOC dynamics may be summarized as follows: (a) in sandy soil, the fine and the medium sand fractions tend to be differentiated by labile OC compounds (O,N-alkyl C and anomeric C), most likely due to the prevalence of immature SOC as characterized by a composition inherited from the plant residues and its fast turnover. (b) Aryl C compounds are not specifically associated with a given soil fraction or

porosity class. These compounds are generally considered recalcitrant, and for this reason, they accumulate in the soil irrespective of the physical fractions. (c) Carbonyl C and alkyl C tend to be associated with the silt–clay fraction of clayey soil (Fig. 5) as a consequence of their interaction with mineral surfaces.

5 Conclusions

Although complex physical, chemical, and biological processes and their interactions govern the SOC turnover, there was evidence that soil porosity distribution could be a valuable indicator of the soil capacity to sequester organic carbon. In particular, in clayey soil, organic compounds were likely protected by the interaction with mineral surfaces and intercalation in phyllosilicates; conversely, low SOC in the sandy soil evidenced a limited SOC protection. In the latter, the high content of labile OC compounds suggested the prevalence of a fast turnover of fresh soil organic matter.

No specific protection mechanisms were identified in the peat soil; conversely, its inherited high SOC content allowed the direct contribution of organic matter to bulk soil porosity to be demonstrated. This research confirms that interactions between soil porosity and organic matter are complex. A number of environmental variables such as long-term fertilization practices may considerably influence the aggregation mechanism and the architecture of pores through the organic matter components. Major progress has been made in the understanding of interactions between aggregates and soil organic matter.

This is evident by continuous evolution of models described for understanding of these interactions.

For management purposes, this study suggests that a rational program of organic fertilization should consider the spatial variability of soil physical properties in order to exploit the capacity of the silt–clay fraction and microaggregates to enhance and protect SOC, in this way increasing the efficiency of the carbon input.

References

Cameron KC, Buchan GD (2006) Porosity and pore size distribution. In: Lal R (ed) Encyclopedia of soil science. CRC Press, Boca Raton, FL, USA

Chen JS, Chiu CY (2003) Characterization of soil organic matter in different particle-size fractions in humid subalpine soils by CP/MAS 13C NMR. Geoderma 117:129–141

Chenu C, Hassink J, Bloem J (2001) Short-term changes in the spatial distribution of microorganisms in soil aggregates as affected by glucose addition. Biol Fertil Soils 34:349–356

Chenu C, Stotzky G (2002) Interactions between microorganisms and soil particles. An overview. In: Huang PM, Bollag JM, Senesi N (eds) Interactions between soil particles and microorganisms. Wiley-VCH-Verlag, Weinheim, pp. 3–39

Christensen BT (2001) Physical fractionation of soil and structural and functional complexity in organic matter turnover. Eur J Soil Sci 52: 345–353

Czarnes S, Hallett PD, Bengough AG, Young IM (2000) Root- and microbial-derived mucilages affect soil structure and water transport. Eur J Soil Sci 51:435–443

Dal Ferro N, Charrier P, Morari F (2013) Dual-scale micro-CT assessment of soil structure in a long-term fertilization experiment. Geoderma 204–205:84–93

Dal Ferro N, Delmas P, Duwig C, Simonetti G, Morari F (2012) Coupling X-ray microtomography and mercury intrusion porosimetry to quantify aggregate structures of a cambisol under different fertilisation treatments. Soil Tillage Res 119:13–21

Derenne S, Largeau C (2001) A review of some important families of refractory macromolecules: composition, origin, and fate in soils and sediments. Soil Sci 166:833–847

Dungait JAJ, Hopkins DW, Gregory AS, Whitmore AP (2012) Soil organic matter turnover is governed by accessibility not recalcitrance. Glob Chang Biol 18:1781–1796

Edwards AM, Phillips RA, Watkins NW, Freeman MP, Murphy EJ, et al. (2007) Revisiting Levy flight search patterns of wandering albatrosses, bumblebees and deer. Nature 449:1044–1048

Elliott ET, Coleman DC (1988) Let the soil work for us. Ecol Bull 39: 23–32

Eusterhues K, Rumpel C, Kogel-Knabner I (2007) Composition and radio C age of HF resistant soil organic matter in a Podzol and a Cambisol. Org Geochem 38:1356–1372

Francioso O, Ferrari E, Saladini M, Montecchio D, Gioacchini P, Ciavatta C (2007) TG-DTA, DRIFT and NMR characterization of humic-like fractions from olive wastes and amended soil. J Hazard Mater 149: 408–417

Francioso O, Montecchio D, Gioacchini P, Cavani L, Ciavatta C, Trubetskoj O, Trubetskaya O (2009) Structural differences of Chernozem soil humic acids SEC–PAGE fractions revealed by thermal (TG–DTA) and spectroscopic (DRIFT) analyses. Geoderma 152:264–268

Freeman C, Ostle NJ, Fenner N, Kang H (2004) A regulatory role for phenol oxidase during decomposition in peatlands. Soil Biol Biochem 36:1663–1667

Grosbellet C, Vidal-Beaudet L, Caubel V, Charpentier S (2011) Improvement of soil structure formation by degradation of coarse organic matter. Geoderma 162:27–38

Hajnos M, Lipiec J, Świeboda R, Sokolowska Z, Witkowska-Walczak B (2006) Complete characterization of pore size distribution of tilled and orchard loamy soil using water retention curve, mercury porosimetry, nitrogen adsorption, and water desorption methods. Geoderma 135:307–314

Haynes RJ, Naidu R (1998) Influence of lime, fertilizer and manure applications on soil organic matter content and soil physical conditions: a review. Nutr Cycl Agroecosyst 51:123–137

Helfrich M, Ludwig B, Buurman P, Flessa H (2006) Effect of land use on the composition of soil organic matter in density and aggregate fractions as revealed by solid-state 13C NMR spectroscopy. Geoderma 136:331–341

Henaut Y, Alauzet C, KLambin M (2002) Effect of starvation on the search path characteristics of Orius majusculus. J Appl Entomol 126:501–503

Hu WG, Mao J, Xing B, Schmidt-Rohr K (2000) Poly(methylene) crystallites in humic substances detected by nuclear magnetic resonance. Environ Sci Technol 34:530–534

Hussein J, Adey MA (1998) Changes in microstructure, voids and b-fabric of surface samples of a Vertisol caused by wet/dry cycles. Geoderma 85:63–82

Jastrow JD, Miller RM (1998) Soil aggregate stabilization and carbon sequestration: feedbacks through organomineral associations. In: Lal R, Kimble JM, Follett RF, Stewart BA (eds) Soil processes and the carbon cycle. CRC Press LLC, Boca Raton, FL, pp. 207–223

Kaiser K, Guggenberger G (2003) Mineral surfaces and soil organic matter. Eur J Soil Sci 54:219–236

Kelleher BP, Simpson MJ, Simpson AJ (2006) Assessing the fate and transformations of plant residues in the terrestrial environment using HR-MAS NMR. Geochim Cosmochim Acta 70: 4080–4094

Khanna M, Yoder M, Calamai L, Stotzky G (1998) X-ray diffractometry and electron microscopy of DNA bond to clay minerals. Sci Soils 3: 1–10

Kuka K, Franko U, Rühlmann J (2007) Modelling the impact of pore space distribution on C turnover. Ecol Model 208:295–306

Lugato E, Simonetti G, Morari F, Nardi S, Berti A, Giardini L (2010) Distribution of organic and humic carbon in wet-sieved aggregates of different soils under long-term fertilization experiment. Geoderma 157:80–85

Lützow MV, Kögel-Knabner I, Ekschmitt K, Flessa H, Guggenberger G, Matzner E, Marschner B (2007) OM fractionation methods: relevance to functional pools and to stabilization mechanisms. Soil Biol Biochem 39:2183–2207

Lützow MV, Kögel-Knabner I, Ekschmitt K, Matzner E, Guggenberger G, Marshner B, Flessa H (2006) Stabilization of organic matter in temperate soils: mechanisms and their relevance under different soil conditions—a review. Eur J Soil Sci 57:426–445

Mafra AL, Senesi N, Brunetti G, Miklós AAW, Melfi AJ (2007) Humic acids from hydromorphic soils of the upper Negro river basin, Amazonas: chemical and spectroscopic characterisation. Geoderma 138:170–176

Mao JD, Fang XW, Schmidt-Rohr K, Carmo AM, Hundal LS, Thompson ML (2007) Molecular-scale heterogeneity of humic acid in particle-size fractions of two Iowa soils. Geoderma 140:17–29

Marschner B, Brodowski S, Dreves A, et al. (2008) How relevant is recalcitrance for the stabilization of organic matter in soils? J Plant Nutr Soil Sci 171:1–110

Morari F, Lugato E, Giardini L (2008) Olsen phosphorus, exchangeable cations and salinity in two long-term experiments of north-eastern

Italy and assessment of soil quality evolution. Agric Ecosyst Environ 124:85–96

Oades JM, Waters AG (1991) Aggregate hierarchy in soils. Aust J Soil Res 29:815–828

Oorts K, Bossuyt H, Labreuche J, Merckx R, Nicolardot B (2007) Carbon and nitrogen stocks in relation to organic matter fractions, aggregation and pore size distribution in no-tillage and conventional tillage in northern France. Eur J Soil Sci 58:248–259

Pagliai M, Vignozzi N, Pellegrini S (2004) Soil structure and the effect of management practices. Soil Tillage Res 79:131–143

Piccolo A (2002) The supramolecular structure of humic substances. A novel understanding of humus chemistry and implications in soil science. Soil Sci 166:810–832

Pituello C, Dal Ferro N, Simonetti G, Berti A, Morari F (2016) Nano to macro pore structure changes induced by long-term residue management in three different soils. Agric Ecosyst Environ 217:49–58

Rao CNR (1963) Chemical applications of infrared spectroscopy. Academic Press, New York

Regelink IC, Cathelijne R, Stoof CR, Rousseva S, Weng L, Lair GJ, Kram P, Nikolaos P, Nikolaidis NP, Kercheva M, Banwart S, Comans RNJ (2015) Linkages between aggregate formation, porosity and soil chemical properties. Geoderma 247–248:24–37

Reynolds PJ, Sharma P, Jenneman GE, McInerney MJ (1989) Mechanisms of microbial movement in subsurface materials. Appl Environ Microbiol 55:2280–2286

Schjønning P, Elmholt S, Munkholm LJ, Debosz K (2002) Soil quality aspects of humid sandy loams as influenced by organic and conventional long-term management. Agric Ecosyst Environ 88:195–214

Schmidt MW, Torn MS, Abiven S, Dittmar T, Guggenberger G, Janssens IA, Kleber M, Kögel-Knabner I, Lehmann J, Manning DA, Nannipieri P, Rasse DP, Weiner S, Trumbore SE (2011) Persistence of soil organic matter as an ecosystem property. Nature 478(7367):49–56

Simonetti G, Francioso O, Nardi S, Berti A, Brugnoli E, Lugato E, Morari F (2012) Characterization of humic carbon in aggregate soil fractions in a long-term experiment with manure and mineral fertilization. Soil Sci Soc Am J 76:880–890

Six J, Bossuyt H, Degryze S, Denef K (2004) A history of research on the link between (micro) aggregates, soil biota, and soil organic matter dynamics. Soil Tillage Res 79:7–31

Six J, Conant RT, Paul EA, Paustian K (2002) Stabilization mechanisms of soil organic matter: implications for C-saturation of soils. Plant Soil 241:155–176

Six J, Paustian K, Elliott ET, Combrink C (2000) Soil structure and organic matter: I. Distribution of aggregate-size classes and aggregate-associated carbon. Soil Sci Soc Am J 64:681–689

StatSoft Inc (2004) STATISTICA, version 7, www.statsoft.com

Strong DT, De Wever H, Merckx R, Recous S (2004) Spatial location of carbon decomposition in the soil pore system. Eur J Soil Sci 4: 739–750

Theng BKG (2007) Formation and Properties of Clay-Polymer Complexes. Elsevier, Amsterdam (1979). doi:10.1002/jpln.19801430317

Van Haastert PJM, Bosgraaf L (2009) Food searching strategy of amoeboid cells by starvation induced run length extension. PLoS One 4(8):6814. doi:10.1371/journal.pone.0006814

Vermeer AWP, Koopal LK (1998) Adsorption of humic acids to mineral particles. 2. Polydispersity effects with polyelectrolyte adsorption. Langmuir 14:4210–4216

Vermeer AWP, van Riemsdijk WH, Koopal LK (1998) Adsorption of humic acid to mineral particles. 1. Specific and electrostatic interactions. Langmuir 14:2810–2819

Walkley A, Black IA (1934) An examination of Degtjareff method for determining soil organic matter and a proposed modification of the chromic acid titration method. Soil Sci 37:29–37

Zaffar M, Lu SG (2015) Pore size distribution of clayey soils and its correlation with soil organic matter. Pedosphere 25:240–249